

Reprinted from *JOURNAL OF CATALYSIS*, Volume 22, Number 3, September 1971  
Copyright © 1971 by Academic Press, Inc. *Printed in U. S. A.*

## Disproportionation of CO

## II. Over Cobalt and Nickel Single Crystals

G. D. RENSHAW,\* C. ROSCOE,† AND P. L. WALKER, JR.

*The Pennsylvania State University, Material Sciences Department,  
University Park, Pennsylvania*

Received December 8, 1970

The catalytic disproportionation of CO in the presence of Ni and Co single crystals has been studied in the temperature range 400-800°C. For both Ni and Co, at the lower temperatures, the formation of an intermediate carbide phase, prior to the formation of carbon which was present mainly in the form of filaments, was shown to be a principal factor. Furthermore, such intermediate carbides often grew in the form of single crystal hexagonal and pseudohexagonal shaped plates. At higher temperatures, a transient carbide phase was predicted to explain the morphology of the finally appearing graphite plates. This graphite displayed physical characteristics typical of a highly crystalline material and was comparable to the graphite formed over heated metals during the pyrolysis of hydrocarbons.

A new form of cobalt carbide,  $\beta$ -Co<sub>3</sub>C, is reported. This has the hexagonal DO<sub>17</sub>-type structure with lattice parameters  $a = 5.26 \text{ \AA}$  and  $c = 8.41 \text{ \AA}$ .

## INTRODUCTION

It was the intent of this study to furnish additional information concerning the nature of the intermediate species, and the morphology of the graphitic products, formed during the catalytic disproportionation of Co over Ni and Co single crystals.

In a similar study using Fe (1), it was found that an oxide,  $\gamma$ -Fe<sub>2</sub>O<sub>3</sub>, constituted the active catalytic species but that carbon finally appeared by way of a series of carbide intermediates. Previous studies (2-4) suggest that the formation of such carbide intermediates, at least, is a necessary prerequisite for the formation of carbon over all three mentioned metals. There is, however, some discrepancy in the liter-

ature concerning the carbides formed by Ni and Co, particularly with regard to their composition, crystal structure, stability, and the temperature range for formation.

For Ni, the carbide, Ni<sub>3</sub>C, has been fairly well established (5). It has a close-packed hexagonal structure which, depending on the method of preparation, decomposes somewhere in the region of 300-450°C (4, 6). Other carbide phases of Ni have also been postulated (7-9).

For Co, the carbide, Co<sub>2</sub>C, was found by Bahr and Jessen (10), and several independent X-ray analyses (11-13) have proved the structure to be orthorhombic. By carburizing Co in the range 450-600°C, Meyer (14) produced a carbide whose diffraction pattern was almost identical with that of cementite, Fe<sub>3</sub>C. Subsequently both Hofer (15) and Drain (16) failed in attempts to produce this same carbide. However, recently Nagakura (3) obtained electron diffraction patterns from carburized Co films which were shown to

\* Present address: United Kingdom Atomic Energy Authority, Atomic Weapons Research Establishment, Aldermaston, Reading RG7 4PR, England.

† Present address: Central Electricity Generating Board, Research Laboratories, Chemistry Division, Capenhurst, Chester, England.

result from a carbide having the cementite structure and almost identical lattice parameters to cementite.

#### EXPERIMENTAL

Details of apparatus and techniques employed in the present study have been described in a previous paper (1).

The nickel single crystal (Metals Research Ltd., England) was in the form of a cylinder having a random orientation. Beams were cut from this crystal, with dimensions  $10 \times 2 \times 2$  mm, having (111) and (110) planes as the two main faces of the beam. The cobalt single crystal (Metals Research Ltd., England) was also in the form of a randomly oriented cylinder, and thin slices for experimentation were cut in a direction perpendicular to the cylinder axis. Both types of crystal were electropolished in a Morris bath followed by a hydrogen treatment at  $600^\circ\text{C}$  prior to reaction. In all experiments the gas employed was a CO-9.4%  $\text{H}_2$  mixture (Matheson Company, Inc., main impurities being 0.018%  $\text{O}_2$  and 0.14%  $\text{CO}_2$ ).

The carbonaceous products were studied in one of two forms; either as bulk products or as a stripped film. Bulk products refer to a large buildup of material on the metal surface; this product material was then removed, ultrasonically dispersed in distilled water, and supported on electron microscope grids. Thin films were stripped from the crystal surface after a reaction time appropriate for preparing specimens suitable for transmission electron microscopy. The films were stripped from the metal by direct chemical attack of the metal substrate using a saturated solution of iodine in 10% potassium iodide. Finally, the film was washed in methanol.

#### RESULTS AND DISCUSSION

##### *Reaction on Nickel*

##### *Stripped Films*

The electron micrograph shown in Fig. 1 depicts the microstructure of the product film formed at  $400^\circ\text{C}$  on a (111) nickel

surface during reaction in a CO-9.4%  $\text{H}_2$  mixture at a pressure of 1 atm for 1 hr. The film has a mosaic appearance and is composed of intergrown and overlapping platelets having an average diameter of ca. 1000 Å. At higher magnification, it is apparent that some of the platelets have a hexagonal morphology (See Fig. 2). Note, also, that such platelets tend to be oriented parallel to one another. Selected area diffraction from the hexagonal plates yielded spot patterns indicating their single crystal nature. Figure 3a shows an example of such a pattern, and an analysis showed that it corresponded to the (0001) reciprocal lattice plane in nickel carbide,  $\text{Ni}_3\text{C}$  (see Fig. 3b). The above observations suggest that the carbide plates bear either an epitaxial or a topotaxial relation to the single-crystal nickel substrate.

Other parts of the film gave selected area diffraction patterns consisting of rings within which individual spots could readily be resolved indicating that the material giving rise to the patterns was polycrystalline and had a crystallite size of the order of a few hundred Angstrom units. The interplanar spacings obtained from such patterns corresponded to graphite. Single-crystal graphite patterns were not observed.

Thin carbonaceous films were also formed on nickel by reacting at a temperature of  $800^\circ\text{C}$  in 1 atm of CO-9.4%  $\text{H}_2$  for periods up to 48 hr. Figure 4 shows an electron micrograph of a film formed in 20 hr on a (111) surface. Individual grains are evident and are demarcated by a network of subgrain boundaries (e.g., A, B, and C). The average grain size is of the order of 2000 Å. At a later stage in the reaction (48 hr) platelike material begins to form in the vicinity of the grain boundaries (see Fig. 5). Selected area diffraction from such plates gave single-crystal spot patterns which on analysis proved to result from a graphite lattice.

The Moiré patterns visible in the electron micrograph of Fig. 6 are the result of the overlapping of two similar lattices with a slight relative disorientation. Bragg diffraction contrast effects are also visible here (and in Fig. 4), e.g., in the region designated

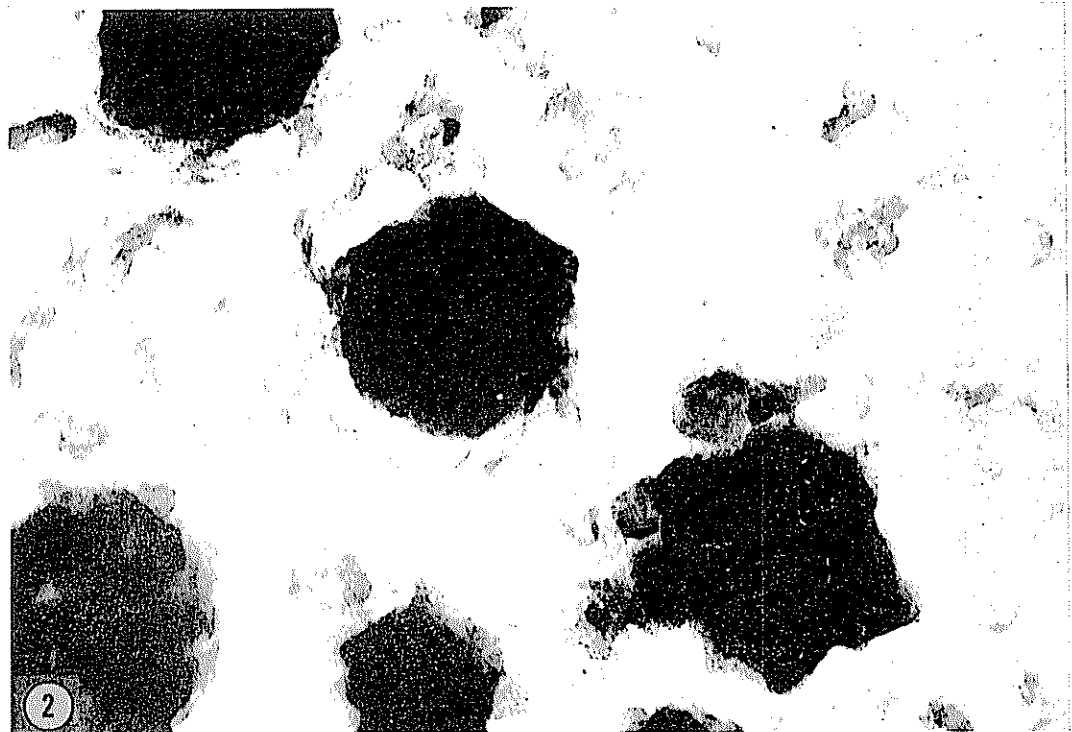
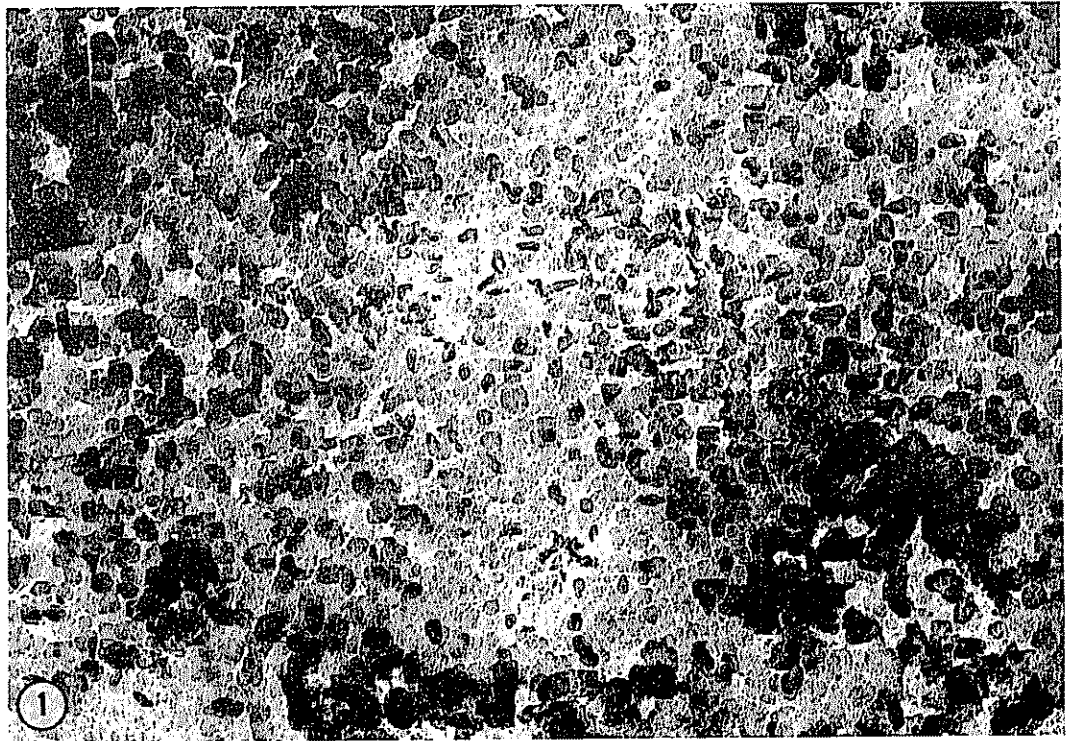


FIG. 1. Transmission electron micrograph showing the film formed on the (111) face of Ni at 400°C in CO-9.4% H<sub>2</sub>. ( $\times 29\ 000$ ).

FIG. 2. Higher magnification micrograph of film depicted in Fig. 1 revealing the hexagonal morphology of the plates. ( $\times 75\ 000$ ).

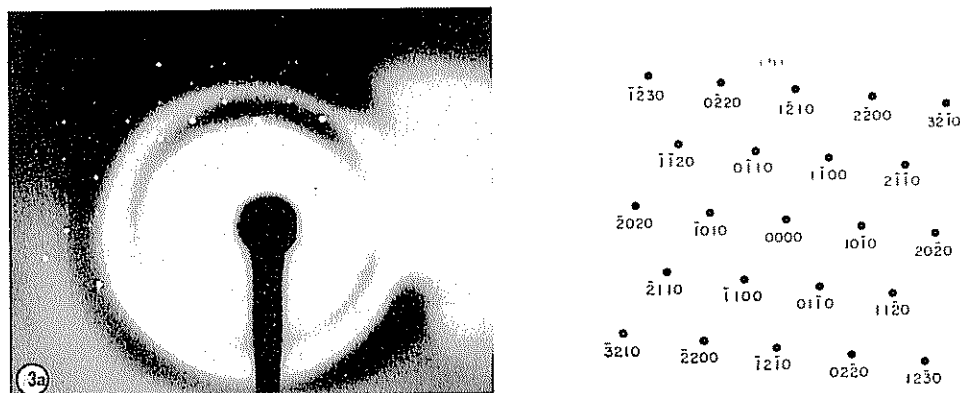


Fig. 3. (a) Selected area diffraction pattern from the plates shown in Fig. 2. (b) The (0001) reciprocal lattice net in Ni<sub>3</sub>C corresponding to the pattern in Fig. 3a.

A and B. Areas of Fig. 6 showing dark contrast most likely contain a small percentage of nickel either as the free metal or in a Ni-C solid solution. Both of these situations could arise from the breakdown of an intermediate carbide phase formed during reaction. The implication of this will be discussed in a later section.

Throughout the product film there appear well-defined hexagonal plates, such as those appearing in the electron micrograph of Fig. 7. Selected area diffraction from such a plate gave the pattern shown in Fig. 8 which was shown to correspond to single crystal graphite oriented with its basal plane parallel to the film surface. It is surprising, considering the relative ease of deformation of graphite crystals, that in all our experiments, basal dislocations were not observed in the graphite crystallites.

Figure 9, which is an electron micrograph, demonstrates the onset of filamentary carbon growth. Again the dark contrast suggests the presence of nickel, formed during carbide decomposition (see later), particularly in the spherical particles to be seen in the lower half of this micrograph.

In Fig. 4, in addition to the network of subgrain boundaries, can be seen another type of growth center within the grains. The electron micrograph of Fig. 10 shows this particular type of growth center more clearly. They have a well-defined square (or sometimes rectangular) outline, and the centers are composed of a faceted region

which could be either a depression or a growth hillock in the stripped film. Selected area diffraction from the central region of the growth center shown in Fig. 10 gave a ring pattern, the  $d$  spacings of which corresponded to polycrystalline graphite. However, since Ni<sub>3</sub>C has some  $d$  spacing close to those of graphite, the possibility that some of the rings correspond to carbide cannot be entirely ruled out. On manipulating the sample so that the electron beam penetrated the outer region of the growth center, a spot pattern appeared together with the ring pattern (see Fig. 11). An analysis showed that the spot pattern resulted from a single-crystal graphite flake oriented with its basal plane parallel to the film surface. From Figs. 10 and 11, a directional relationship between the graphite and the growth center may be deduced. The edge of the growth center was found to be parallel to the  $\langle 2\bar{1}10 \rangle$  direction in the graphite lattice, that is, the so-called arm-chair direction.

The perfection of the graphite formed is comparable to that produced during the pyrolysis of hydrocarbons over heated metal substrates (17, 18), suggesting a possible similarity in the mode of formation. Recently Presland *et al.* (19) pyrolyzed acetylene over Ni single crystals at 1000°C and demonstrated that single crystal graphite was produced on the (110) face, whereas on the (111) face the graphite tended to be polycrystalline. In the present

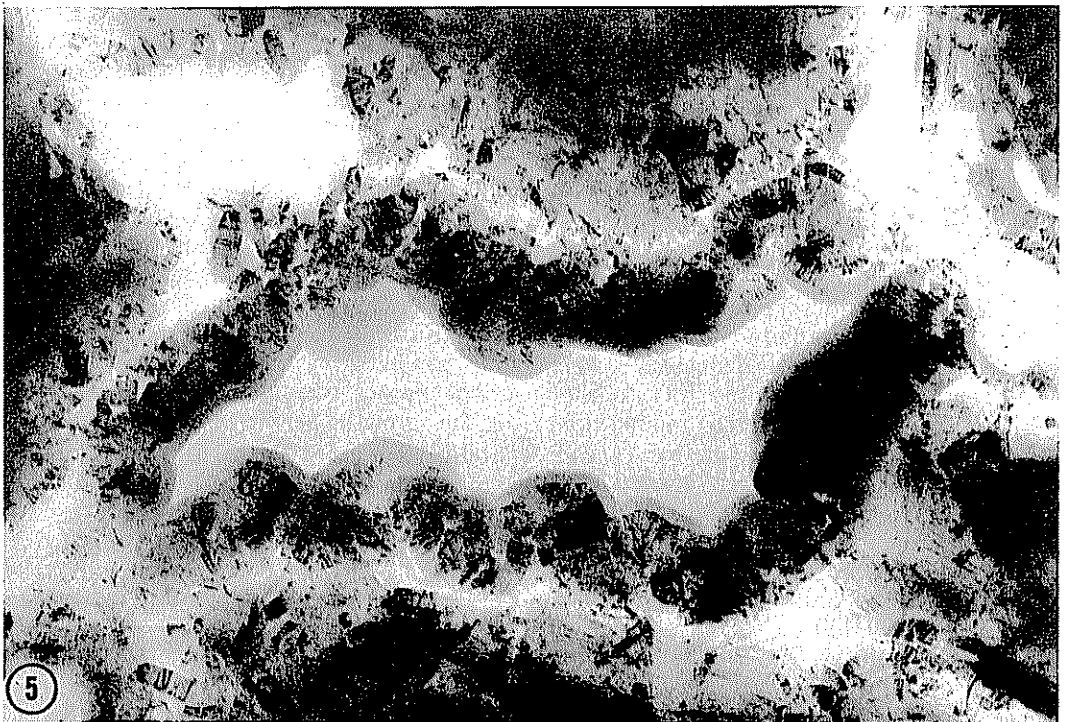
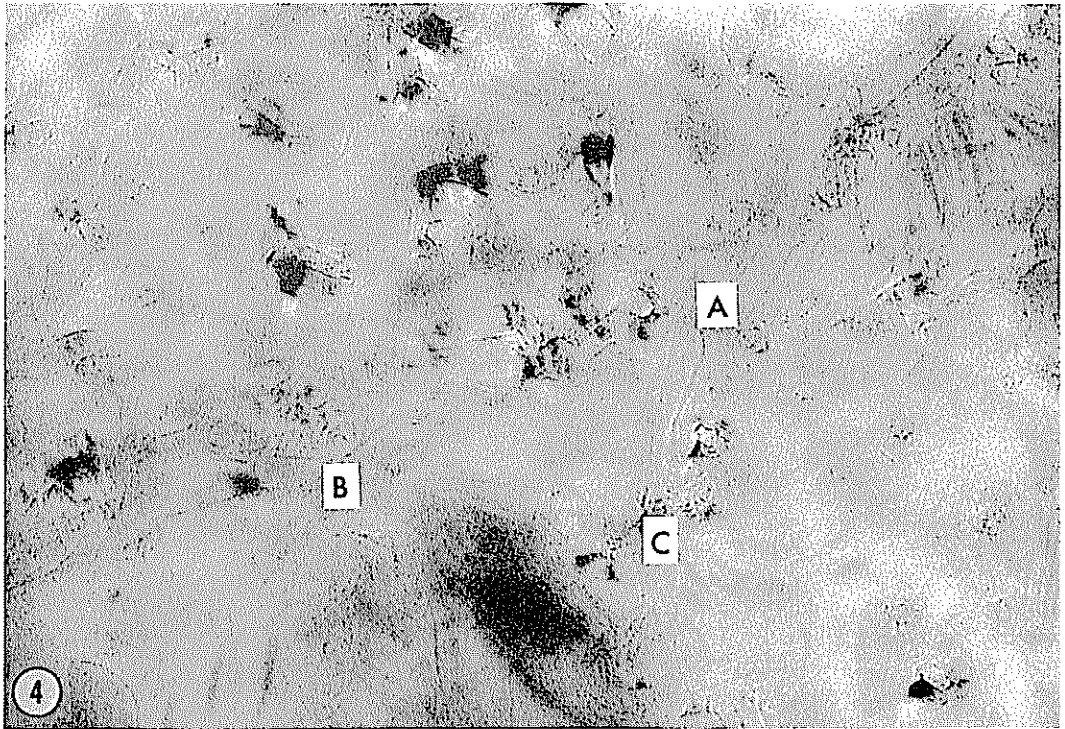


FIG. 4. Transmission electron micrograph showing the film formed on the (111) face of Ni at 800°C in CO-9.4% H<sub>2</sub>. Note the subgrain boundary ABC. ( $\times 114\ 000$ ).

FIG. 5. Transmission electron micrograph showing platelike material growing at the grain boundary. ( $\times 49\ 000$ ).

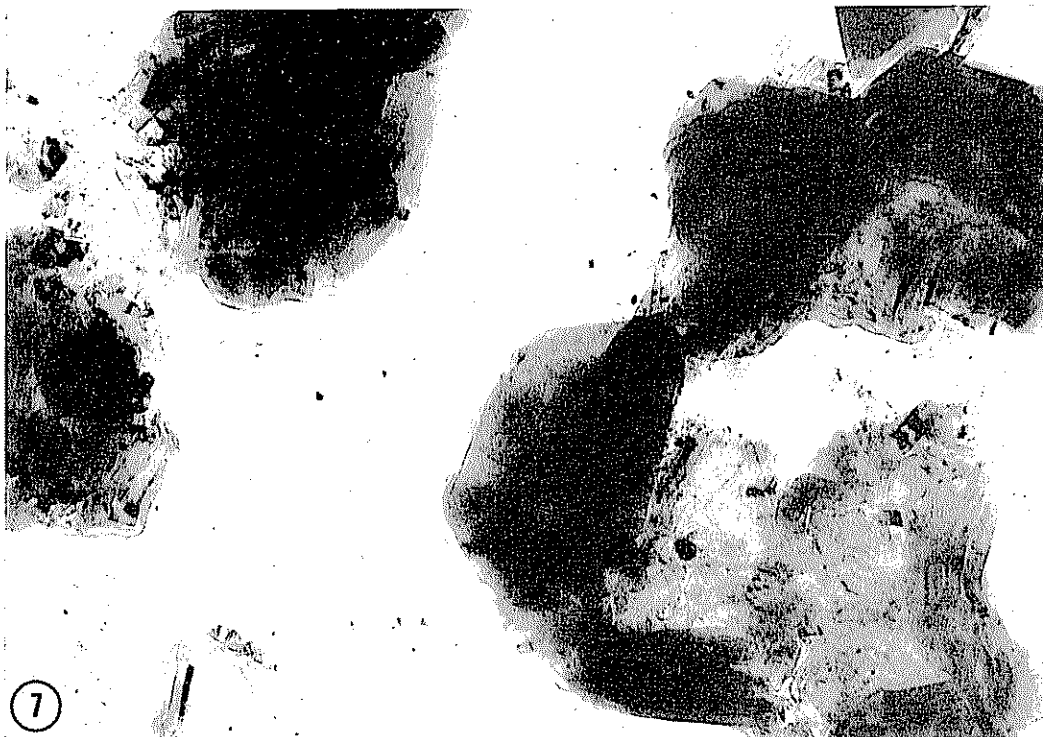
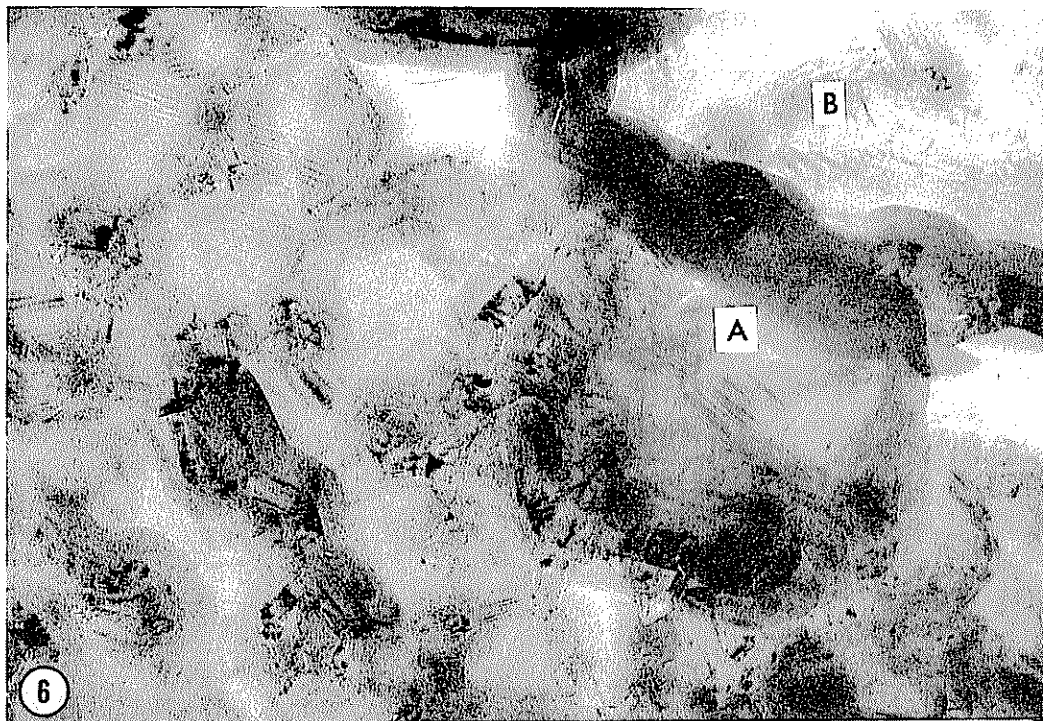


FIG. 6. Moiré patterns and Bragg diffraction contrast effects (see areas A and B) in the film formed on Ni at 800°C in CO-9.4% H<sub>2</sub>. Transmission electron micrograph. (×49 000).

FIG. 7. Hexagonal shaped plates in the film formed in the (111) face of Ni at 800°C in CO-9.4% H<sub>2</sub>. Transmission electron micrograph. (×39 000).

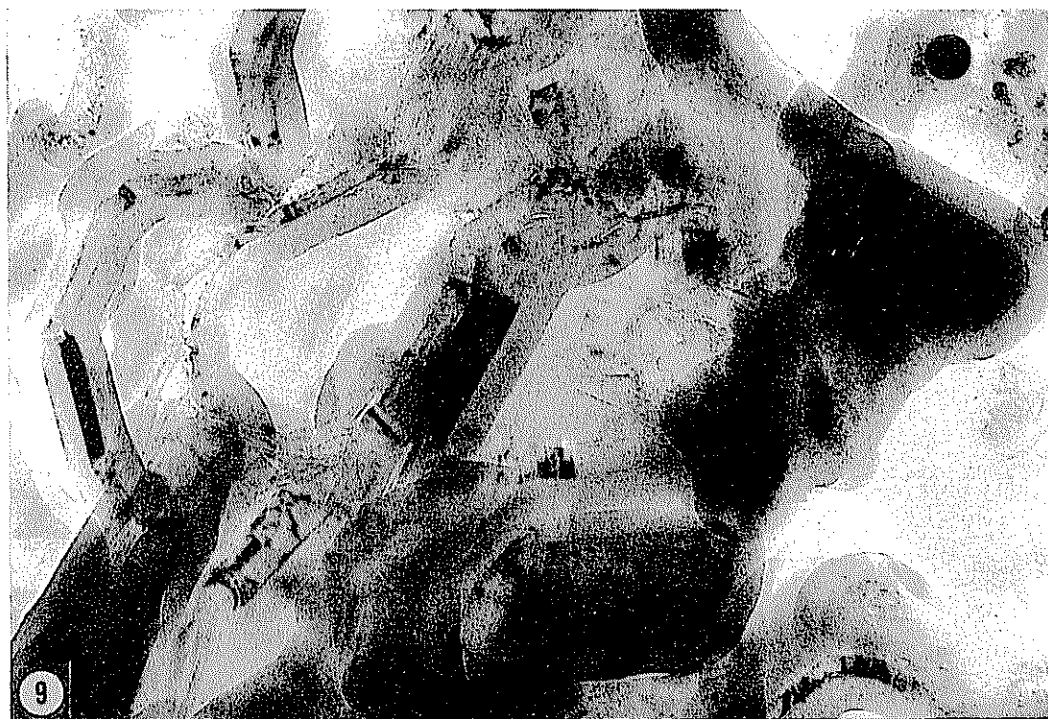


FIG. 8. Selected area diffraction pattern from plates in Fig. 7 corresponding to single crystal graphite. Beam perpendicular to (0001) plane.

FIG. 9. Transmission electron micrograph depicting the onset of growth of carbon filaments on Ni at 800°C. ( $\times 49\,000$ ).



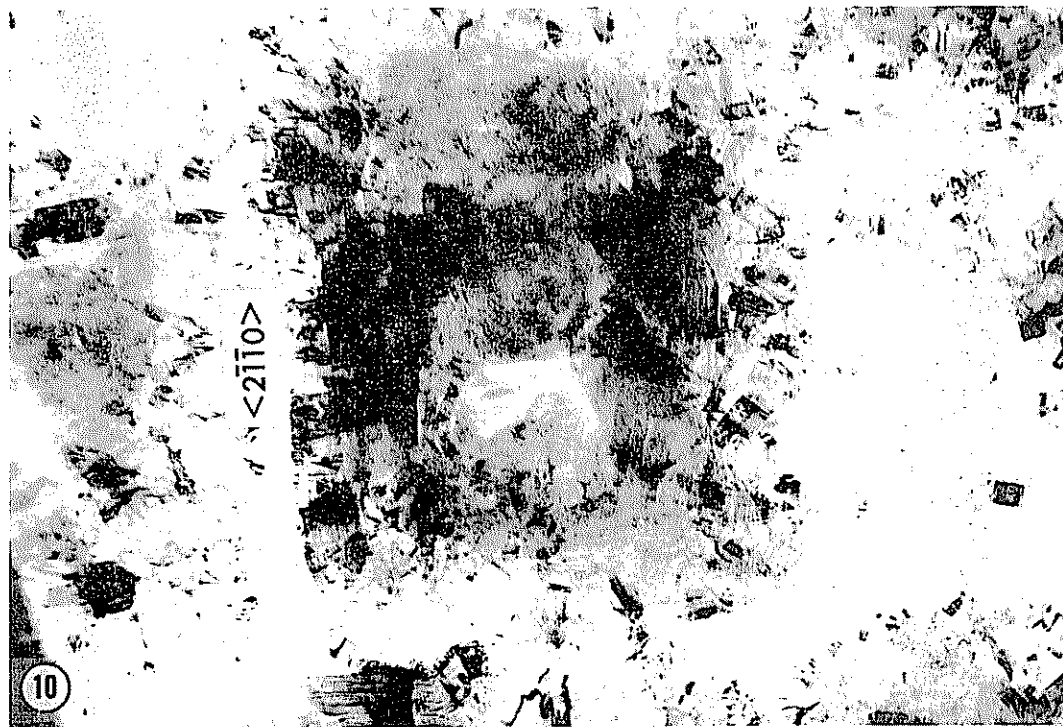


Fig. 10. Growth center in Ni reacted at 800°C in CO-9.4% H<sub>2</sub>. Note the square outline and the facets within the growth feature. ( $\times 49\,000$ ).

study single crystal graphite was formed on both faces.

#### *Bulk Products*

Samples were taken from the products formed on a crystal reacted in 1 atm of CO-9.4% H<sub>2</sub> for 30 hr at 550°C, the optimum temperature for the fastest rate of product growth. Observation in the electron microscope revealed the carbonaceous products typical of this reaction (20), namely, a platelike material and a highly fibrous material (see Fig. 12).

Selected area diffraction of the platelike material sometimes gave rise to single-crystal spot patterns such as the one shown in Fig. 13a. This pattern has been indexed and shown to correspond to the (03 $\bar{3}$ 1) reciprocal lattice plane in Ni<sub>3</sub>C (see Fig. 13b). The dimensions of the plates was comparable to those found in the stripped films at 400°C. This suggests that, as the reaction progresses, the surface film continually breaks up mechanically and the

resulting individual plates are carried into the bulk products by the growing filaments.

More commonly, the selected area diffraction patterns from the filamentary material were composed of rings which were found to correspond to reflections in the graphite lattice. As for those formed when Fe is employed as the catalyst, many of the filaments were hollow. It has been proposed (1) that the growth of Fe<sub>3</sub>C whiskers is a precursor to the formation of carbon filaments in the presence of Fe. The frequent observation of well-defined carbide crystals embedded in the filaments provided some of the support for this viewpoint. However, although searched for, no evidence of this nature has been found for the formation of analogous nickel carbide whiskers.

#### *Structure of Nickel Carbide*

From X-ray diffraction data, Jacobson and Westgren (5) proposed a close-packed hexagonal structure for Ni<sub>3</sub>C having the

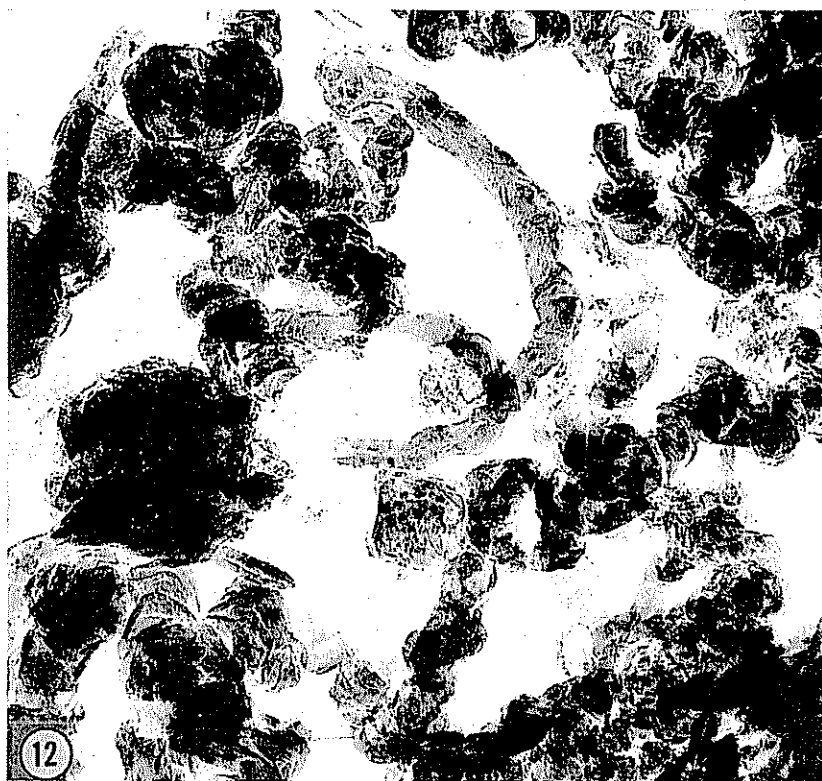
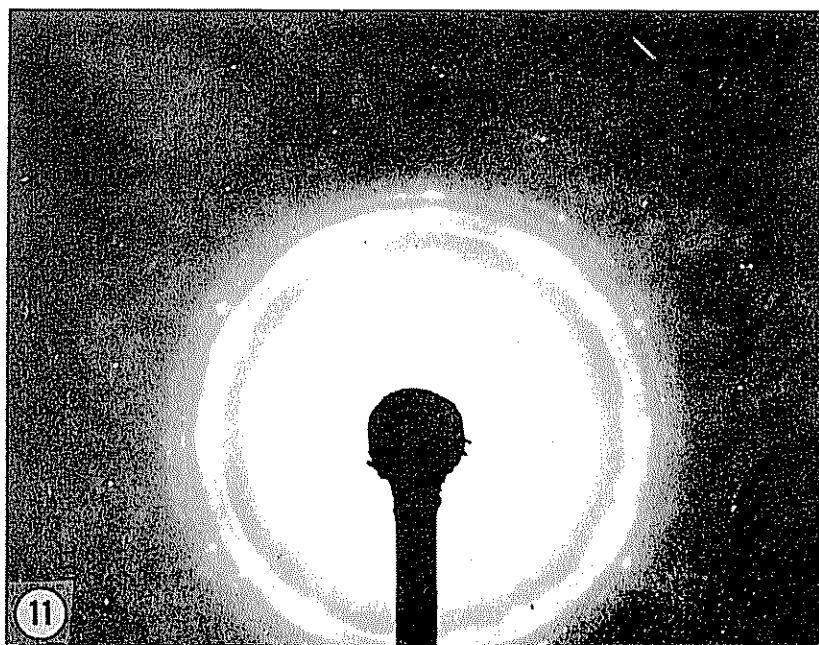


FIG. 11. Selected area diffraction patterns from an area encompassing the growth center shown in Fig. 10. Beam perpendicular to (0001) plane.

FIG. 12. Carbonaceous bulk products formed on Ni during reaction in CO-9.4% H<sub>2</sub> at 550°C. Transmission electron micrograph. ( $\times 24\,000$ ).

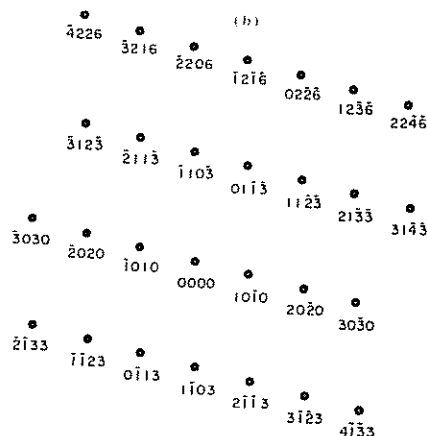
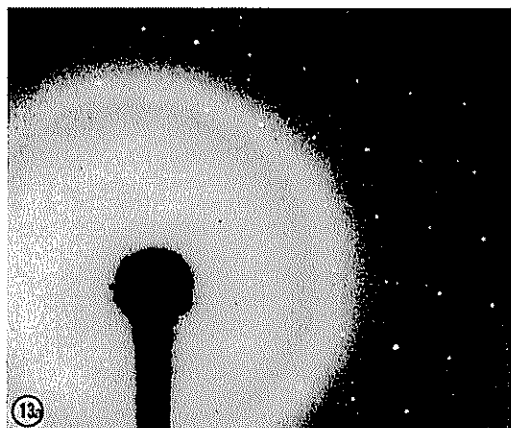


Fig. 13. (a) Typical selected area diffraction pattern from the platelike material shown in Fig. 12. (b) The (03 $\bar{1}$ 1) reciprocal lattice net in Ni<sub>3</sub>C corresponding to the pattern shown in Fig. 13a.

lattice constants,  $a_h = 2.649 \text{ \AA}$ ,  $c_h = 4.238 \text{ \AA}$ , and  $c_h/a_h = 1.636$ . The electron diffraction patterns obtained in the present study (see, e.g., Fig. 3a), however, are not in accord with this unit cell but instead provide confirmation for the existence of the superlattice proposed by Nagakura (4). The lattice constants for this superlattice, which is based on the Jacobson and Westgren cell, are  $a = \sqrt{3} a_h = 4.553 \text{ \AA}$  and  $c = 3c_h = 12.92 \text{ \AA}$ . In the superlattice the nickel atoms occupy the same positions as in the Jacobson and Westgren cell. However, the carbon atoms now exhibit a regular arrangement, that is, they are now ordered.

#### Mechanism

The observations described in the preceding sections suggested to us that carbon formation at temperatures below 550°C results from the decomposition of the precursor carbide, Ni<sub>3</sub>C, which becomes metastable above ca. 300°C (21). No diffraction data were obtained to support the premise that a carbide phase formed at higher temperatures. There are, however, at least two observations which strongly suggest that reaction does proceed via an intermediate phase. First, the average grain size is much larger in films grown at 800°C, relative to those grown at 400°C. It is inconceivable that graphite could undergo such a recrystallization at these temperatures. Secondly, the hexagonally

shaped graphite single crystals, which are a feature of the reaction of 800°C, are very reminiscent of the single-crystal carbide plates formed below 550°C. The possibility that the onset of growth of graphite crystals coincides with the formation of a carbide other than Ni<sub>3</sub>C cannot be rejected. It is particularly noteworthy that Lonsdale *et al.* (22) have reported evidence for believing that transient carbides are important in the growth of diamonds from Ni-C solutions.

The intermediate carbide phase could result by reaction, probably topotactic, between the active carbon atoms, generated during the disproportionation, of carbon monoxide, and either Ni or NiO. Although there is no direct evidence for the formation of an oxide film, the subgrain boundaries and growth centers (see Figs. 4 and 10) observed in this study strongly resemble the features noted by Wood *et al.* (23) during a study of the oxidation of Ni at 1200°C. For this reason the oxide, rather than the metal, may be the active catalytic species involved in the disproportionation of CO.

#### Reaction on Cobalt

##### Stripped Films

A cobalt crystal was reacted at 700°C for 1 hr in CO-9.4% H<sub>2</sub> at a pressure of 1 atm. The stripped product film was shown in the electron microscope to be composed pre-

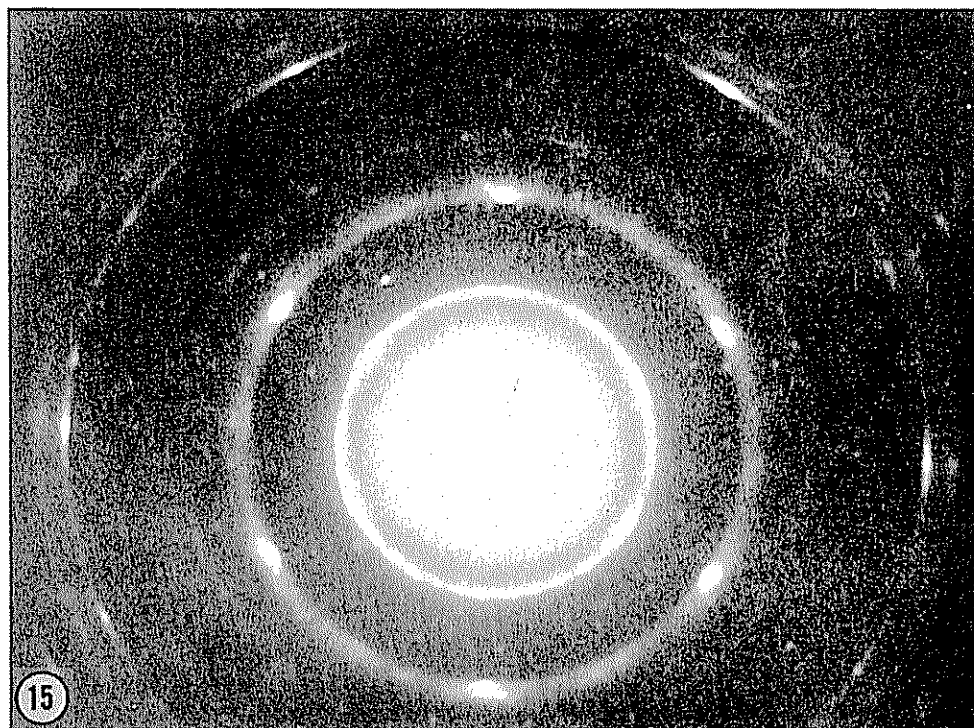
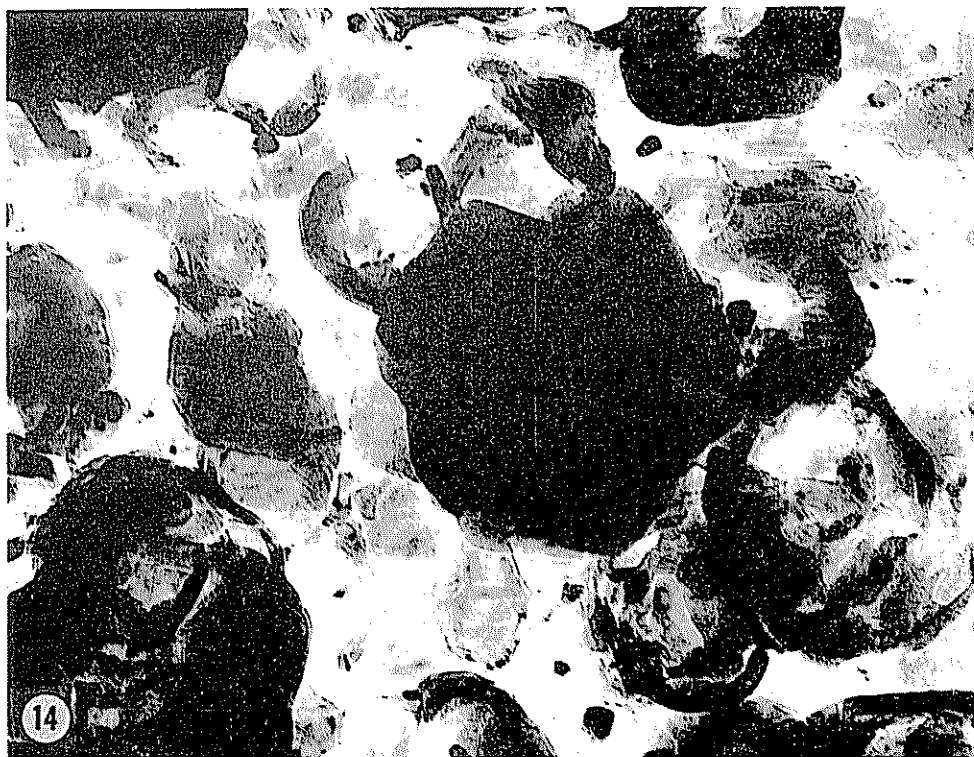


Fig. 14. Typical hexagonal plate observed in the film stripped from a Co single crystal reacted in CO-9.4% H<sub>2</sub> at 700°C. Transmission electron micrograph. ( $\times 115\ 000$ ).

Fig. 15. Selected area diffraction pattern obtained from the area depicted in Fig. 14. Beam perpendicular to (0001) plane.

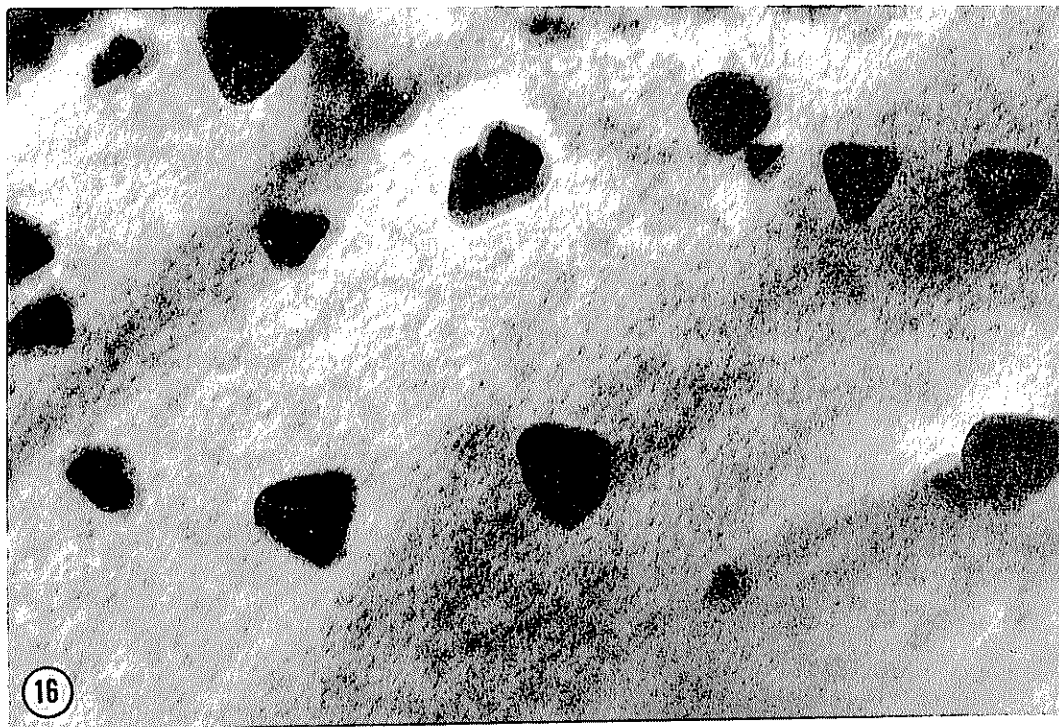


FIG. 16. Transmission electron micrograph of film formed on Co crystal, reacted in CO-9.4% H<sub>2</sub> at 700°C, depicting triangular shaped growth features. ( $\times 74\ 000$ ).

FIG. 17. Flat ribbed plate observed in the bulk products formed over Co at 450°C during reaction in CO-9.4% H<sub>2</sub>. Transmission electron micrograph. ( $\times 74\ 000$ ).

dominantly of platelike material, with many of the plates exhibiting a very well-defined hexagonal morphology. A typical hexagonal plate is shown in Fig. 14. The selected area diffraction depicted in Fig. 15 is typical of that obtained from most areas of the sample and was shown to result from graphite oriented with its basal plane parallel to the film surface. This was revealed by the appearance of sharp spots, lying on the rings (produced by polycrystalline graphite) in the diffraction pattern, expected from the (0001) reciprocal lattice plane in graphite.

Electron diffraction failed to produce any evidence that would indicate the presence of either a carbide or oxide phase at this temperature. However, when the electron beam was centered on the triangular shaped nuclei shown in Fig. 16, so as to obtain selected area diffraction, they appeared to decompose suggesting that they were not composed purely of carbon. The pronounced outer shell surrounding most of the nuclei also suggests that the decomposition of a carbide phase had occurred.

#### Bulk Products

The results in this section represent a study of the bulk products formed on cobalt during reaction at 450°C in CO-9.4% H<sub>2</sub> at 1 atm pressure for 20 hr. The carbonaceous products were found to consist

of a mixture of plates, essentially of two types, and filaments with some of the filaments appearing hollow and others twisted into a rope-like conformation. The electron micrograph of Fig. 17 depicts a commonly observed growth phenomenon. Here the product has taken the form of a flat, ribbed plate. It is possible that this ribbed structure resulted from the decomposition and breakup of a carbide film. As in the case for nickel, no well-formed single crystal inclusions, such as those observed by Hofer *et al.* (20), were found in the filaments.

Selected area diffraction of the products proved that most, but not all, of the plate and filamentary material was composed of polycrystalline graphite. Single-crystal graphite flakes were occasionally found, as revealed by spot patterns such as the one shown in Fig. 18a (the ring pattern here corresponds to the aluminum standard). The corresponding (01 $\bar{1}$ 1) reciprocal lattice net is shown in Fig. 18b. This is a particularly significant observation since the temperature of formation is only 450°C.

Within the products many hexagonal and pseudo-hexagonal shaped plates were observed (see Fig. 19). The pseudo-hexagonal plate in Fig. 19, when subjected to selected area diffraction, gave the spot pattern shown in Fig. 20a. From a detailed analysis of this and other patterns obtained from

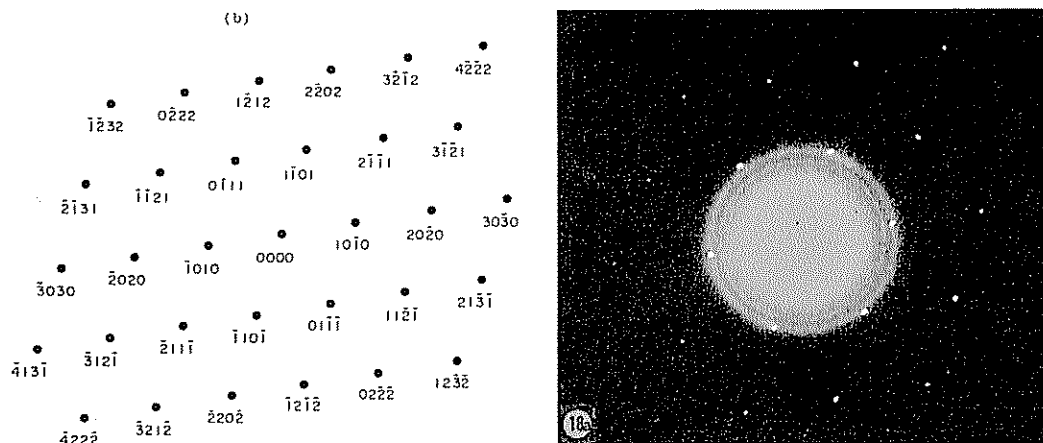


FIG. 18. (a) Selected area diffraction pattern from a graphite flake formed on Co at 450°C during reaction in CO-9.4% H<sub>2</sub>. (b) The (01 $\bar{1}$ 1) reciprocal lattice net in graphite corresponding to the diffraction pattern shown in Fig. 18(a).

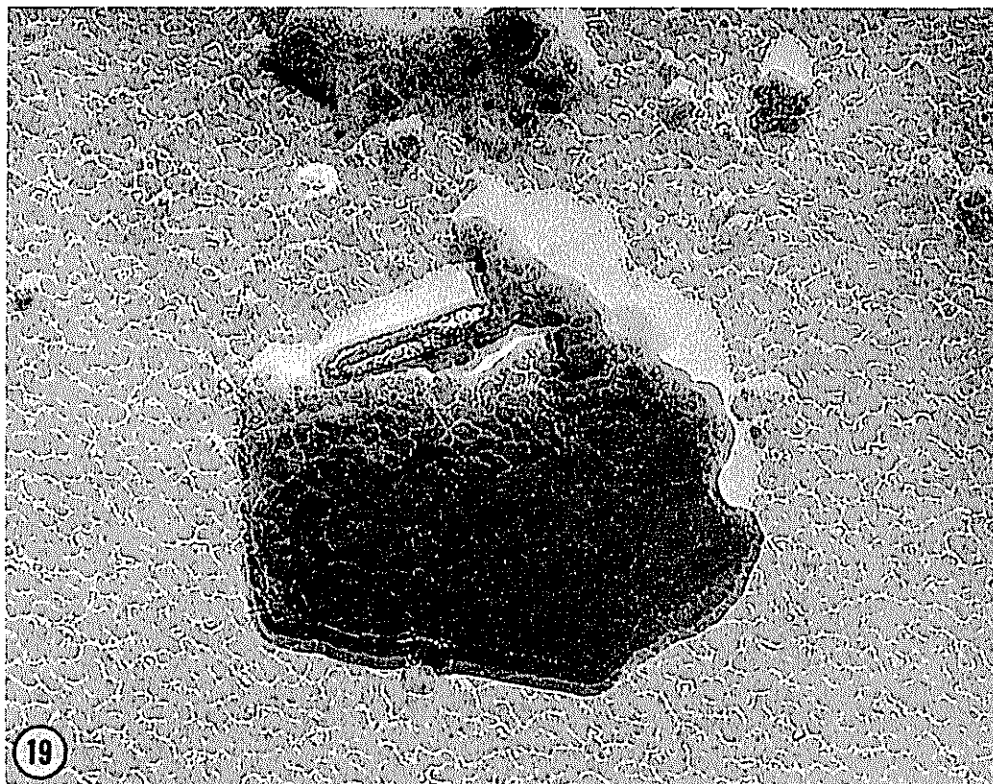


Fig. 19. Transmission electron micrograph showing hexagonal shaped plates in the bulk products formed during the reaction of Co with CO-0.4% H<sub>2</sub> at 450°C. ( $\times 74\,000$ ).

different orientations of the crystal, together with a consideration of the possible structures that could be assigned, it was concluded that the plates were composed of cobalt carbide, Co<sub>3</sub>C, having a hexagonal

unit cell. It follows that the pattern of Fig. 20a represents the (0001) reciprocal lattice plane (see Fig. 20b). This carbide has not been previously reported and has been designated  $\beta$ -Co<sub>3</sub>C in order to dis-

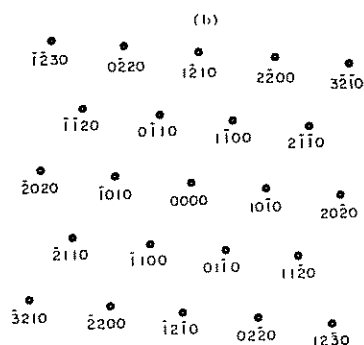
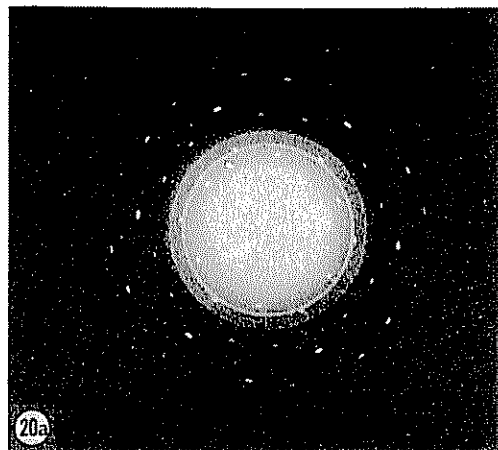


Fig. 20. (a) Selected area diffraction pattern obtained from the plates shown in Fig. 19. (b) The (0001) reciprocal lattice net in  $\beta$ -Co<sub>3</sub>C corresponding to the diffraction pattern shown in Fig. 20a.

tinguish it from the other known form of  $\text{Co}_3\text{C}$  which is now termed  $\alpha\text{-Co}_3\text{C}$ .

The other type of platelike material is typified by the electron micrograph of Fig. 21. All such plates has a characteristic envelope of less-crystalline material surrounding an inner nucleus which is relatively more crystalline (as revealed in dark field in the electron microscope). Some of them, such as the one shown in Fig. 21, exhibit angles between segments of the plate which are the same as the angles characteristic of the hexagonal plates discussed in the previous paragraph. Electron diffraction showed these plates to be composed of graphite.

#### *Structure of Cobalt Carbide*

An evaluation of the diffraction patterns from the hexagonal and pseudohexagonal plates (see Fig. 19) demonstrated that they consisted of a form of  $\text{Co}_3\text{C}$  having a hexagonal unit cell. The known form of  $\text{Co}_3\text{C}$

has an orthorhombic unit cell with lattice constant  $a = 4.483 \text{ \AA}$ ,  $b = 5.033 \text{ \AA}$ , and  $c = 6.731 \text{ \AA}$ , and is isomorphous with cementite,  $\text{Fe}_3\text{C}$ . The symmetrically disposed hexagonal array of spots of the diffraction pattern shown in Fig. 20a normally could never be produced by a crystal having an orthorhombic unit cell with the parameters listed above. However, Ruedl and Amelinckx (24) recently reported an electron diffraction pattern from  $\text{Ni}_3\text{Mo}$ , which is orthorhombic and has the lattice parameters  $a$  and  $b$  within less than 1% of the corresponding  $a$  and  $b$  parameters for  $\text{Co}_3\text{C}$  (orthorhombic), having a symmetrically disposed hexagonal array of spots. They indexed the possible spots resulting from an orthorhombic unit cell and explained the extra spots as resulting from antiphase boundaries and twins in the substructure caused by ordering. Thus, by employing a similar argument, we could have concluded that the pattern in Fig. 20a corresponded

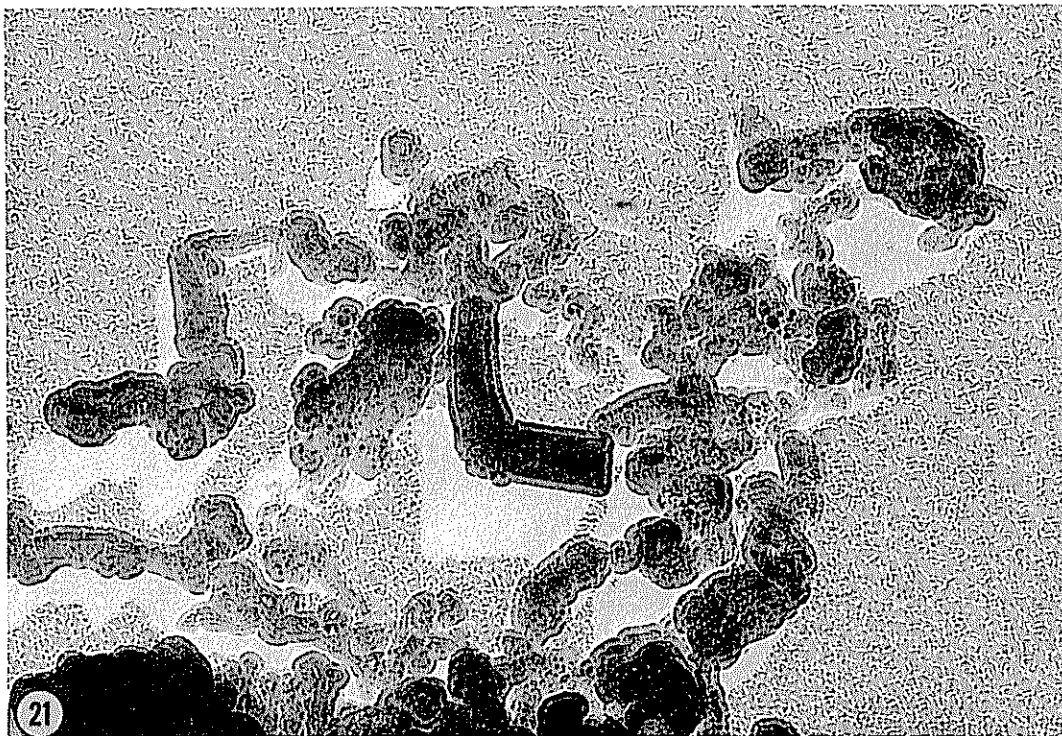


FIG. 21. Transmission electron micrograph of carbonaceous products from the reaction of  $\text{Co}$  with  $\text{CO}-9.4\% \text{ H}_2$  at  $450^\circ\text{C}$ . Note the characteristic envelope (appears lighter) surrounding each piece of material. ( $\times 74\ 000$ ).



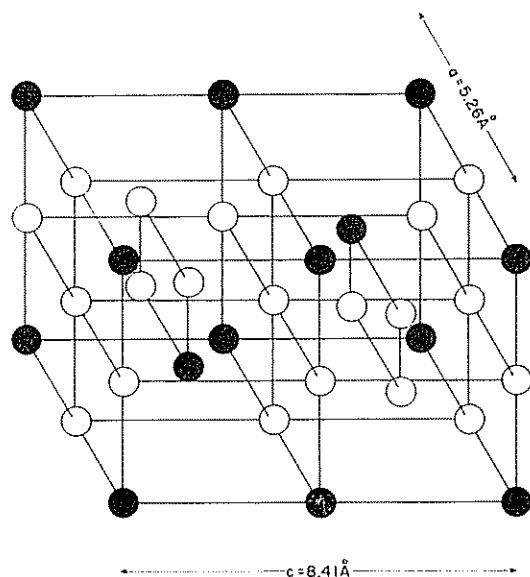


FIG. 22. Hexagonal unit cell for  $\beta$ - $\text{Co}_3\text{C}$ . ●, carbon atoms; ○, cobalt atoms.

to the form of  $\text{Co}_3\text{C}$  previously identified exhibiting an orthorhombic unit cell. If, on the other hand, we index the pattern of Fig. 20a assuming a hexagonal unit cell, we can assign a (0001) reciprocal lattice (see Fig. 20b). By reference to Fig. 20b it can be seen, e.g., that rotation of the crystal about the  $\langle 21\bar{1}0 \rangle$  axis will enable us to obtain the (12 $\bar{3}$ 1) reciprocal plane in a hexagonal lattice. This pattern was indeed found in practice and, therefore, proved conclusively that the plates had a hexagonal crystal structure.

The measured lattice parameters were  $a = 5.26 \text{ \AA}$  and  $c = 8.41 \text{ \AA}$ . The  $a$  parameter was measured directly from the pattern shown in Fig. 18a and the  $c$  parameter was obtained by finding, by trial and error, the best value of  $c$  for all the observed reflections and interplanar spacings in the (1 $^2$ 1) reciprocal lattice plane.

The axial ratio,  $c/a$ , is close to 1.63 and the observed lattice parameters are representative of the group of compounds,  $\text{M}_3\text{X}$ , with the hexagonal  $\text{DO}_{19}$ -type structure (25). The proposed structure for  $\beta$ - $\text{Co}_3\text{C}$  is illustrated in Fig. 22, where the individual atoms have the following positions:

$$\begin{aligned} \text{C}_I & 0,0,0; 0,0,1/2. \\ \text{C}_{II} & 1/3,2/3,1/4; 2/3,1/3,3/4. \\ \text{Co}_I & 1/2,0,0; 0,1/2,0; 1/2,1/2,0; 1/2,0,1/2; \\ & 0,1/2,1/2; 1/2,1/2,1/2. \\ \text{Co}_{II} & x,2x,1/4; 2\bar{x},\bar{x},1/4; x,\bar{x},1/4; \\ & \bar{x},2\bar{x},3/4; 2x,x,3/4; \bar{x},\bar{x},3/4. \end{aligned}$$

where  $x = 0.833$ .

### Mechanism

The mode of the disproportionation of CO over cobalt single crystals parallels quite closely the sequence of reactions on nickel, particularly with regard to the morphology of the products. At  $450^\circ\text{C}$ , hexagonal shaped  $\text{Co}_3\text{C}$  plates are formed which are morphologically the same as the graphite plates observed at  $700^\circ\text{C}$ . This suggests the formation of a transient carbide prior to graphite growth. Perhaps more convincing evidence for the existence of a carbide precursor at  $700^\circ\text{C}$  is forthcoming from the observed decomposition of the triangular shaped nuclei (see Fig. 16) in the electron beam.

From thermodynamic considerations the experimental conditions were such that an oxide film could have formed on the cobalt surface prior to carbide formation. However, neither diffraction patterns from cobalt oxides nor topographical features of the stripped film corresponding to growth features characteristic of cobalt oxides were observed.

### CONCLUSIONS

1. In the disproportionation of carbon monoxide over both Ni and Co, at the lower temperatures, the formation of an intermediate carbide phase, prior to carbon formation, was shown to be a principal factor. Furthermore, such intermediate carbides tend to grow in the form of hexagonal and pseudo-hexagonal shaped plates often exhibiting a single crystal character.

2. The bulk carbonaceous products on both metals consist of platelike and filamentary material.

3. The graphite formed at higher temperatures displayed physical characteristics typical of a highly crystalline material and was comparable to the graphites formed

over heated metals during the pyrolysis of hydrocarbons.

4. At the higher temperatures, where presumably cobalt and nickel carbides are metastable, an intermediate transient carbide phase, which may or may not be related to the carbide produced at the lower temperatures, was predicted to explain the morphology of the graphite plates.

5. A new form of cobalt carbide,  $\beta$ -Co<sub>3</sub>C, has been reported having the hexagonal DO<sub>24</sub>-type structure with lattice parameters  $a = 5.26 \text{ \AA}$  and  $c = 8.41 \text{ \AA}$ .

#### REFERENCES

1. RENSCHAW, G. D., ROSCOE, C., AND WALKER, P. L., JR., *J. Catal.* **18**, 164 (1970).
2. NAGAKURA, S., *J. Phys. Soc. Jap.* **14**, 186 (1959).
3. NAGAKURA, S., *J. Phys. Soc. Jap.*, **12**, 482 (1957).
4. NAGAKURA, S., *J. Phys. Soc. Jap.* **16**, 1213 (1961).
5. JACOBSON, B., AND WESTGREN, A., *Z. Physik. Chem. B* **20**, 361 (1933).
6. HOFER, L. J. E., COHN, E. M., AND PEBBLES, W. C., *J. Phys. Colloid Chem.* **54**, 1161 (1950).
7. TEBBOTII, J. A., *J. Soc. Chem. Ind.* (London) **67**, 62 (1948).
8. TUTIYA, H., *Bull. Mat. Phys. Chem. Research* (Tokyo) **10**, 951 (1931).
9. KOHLHASS, R., AND MEYER, W. F., *Metalwirt. Metallwiss., Metalltech.* **17**, 786 (1938).
10. BAHR, H. A., AND JESSEN, V., *Ber. Bunsenges. Phys. Chem.* **63B**, 2226 (1930).
11. CLARK, J., AND JACK, K. H., *Chem. Ind., London*, 1004 (1951).
12. DRAIN, J., AND MICHEL, A., *Bull. Soc. Chim. Fr.*, 23 (1951).
13. JUZA, R., AND PUFF, H., *Naturwissenschaften* **38**, 331 (1951).
14. MEYER, W. F., *Z. Kristallogr., Kristallgeometric, Kristallphys.* **97**, 145 (1937).
15. HOFER, L. J. E., *Catalysis* **4**, 403 (1956).
16. DRAIN, J., *Ann. Chim. (Paris)* **8**, 900 (1953).
17. PRESLAND, A. E. B., AND WALKER, P. L., JR., *Carbon (Oxford)* **7**, 1 (1969).
18. ROBERTSON, S. D., *Nature, London* **221**, 1044 (1969).
19. PRESLAND, A. E. B., ROSCOE, C., AND WALKER, P. L., JR., "Proceedings of the Third Conference on Industrial Carbon and Graphite," Society of Chemical Industry, in press.
20. HOFER, L. J. E., STERLING, E., AND MCCARTNEY, J. T., *J. Phys. Chem.* **59**, 1153 (1955).
21. HANSEN, M., "Constitution of Binary Alloys," p. 374. McGraw-Hill, 1958.
22. LONSDALE, K., MILEDGE, H. J., AND NAVE, E., *Mineral. Mag.* **32**, 185 (1959).
23. WOOD, G. C., FERGUSON, J. M., VASZKO, B., AND WHITTLE, D. P., *J. Electrochem. Soc.* **114**, 535 (1967).
24. RUEDL, E., AND AMELINCKX, S., *Mater. Res. Bull.* **4**, 361 (1969).
25. PEARSON, W. B., "Handbook of Lattice Spacings and Structures of Metals," p. 106. Pergamon Press, 1958.